Received: 16 November 2021 | Revised: 19 December 2021 | Accepted: 19 December 2021

DOI: 10.1002/bkcs.12463

ARTICLE

BKCS BULLETIN OF THE KOREAN CHEMICAL SOCIETY

Solvation structure of phosphonium ionic liquid/CH_3SCN mixture as electrolytes for Li-ion batteries: Infrared pump-probe spectroscopic studies

Prabhat Kumar Sahu[1] | **Jungyu Kim**[1,2] | **Kwanghee Park**[1] | **Eunchan Kim**[1,2] | **Saptarsi Mondal**[1] | **Kyungwon Kwak**[1,2] | **Minhaeng Cho**[1,2]

[1]Center for Molecular Spectroscopy and Dynamics, Institute for Basic Science (IBS), Korea University, Seoul, South Korea

[2]Department of Chemistry, Korea University, Seoul, South Korea

Correspondence
Kyungwon Kwak and Minhaeng Cho, Center for Molecular Spectroscopy and Dynamics, Institute for Basic Science (IBS), Korea University, Seoul 02841, South Korea.
Email: kkwak@korea.ac.kr and mcho@korea.ac.kr

Funding information
National Research Foundation of Korea, Grant/Award Number: NRF-2020R1A5A1019141; Institute for Basic Science, Grant/Award Number: IBS-R023-D1

Abstract

Lithium-ion battery (LIB) electrolytes based on room-temperature ionic liquids (RTIL) are promising as safe and sustainable LIB electrolytes. However, there are no reports on the solvation structure and dynamics of RTIL due to the existence of various solvation species in RTIL. Here, we investigated the solvation structure and dynamics of binary mixtures of the phosphonium ionic liquid, tributyl (2-methoxyethyl)phosphonium bis(trifluoromethanesulfonyl)imide (P_{444102}TFSI), and methylthiocyanate (CH_3SCN), with ultrafast mid-IR Spectroscopy. The changes of vibrational and rotational dynamics of $CH_3SCN\cdots Li^+$ complex and free CH_3SCN with an increase in CH_3SCN concentration suggest the presence of at least four solvation species, providing superior resolving power for various solvation species existing in complex LIB electrolytes. Our experimental results show that the environment of free CH_3SCN and $CH_3SCN\cdots Li^+$ complex changes drastically with change in CH_3SCN mole fraction and Li salt concentration in the mixture. We expect that this can affect the Li-ion transport mechanism in the IL-based electrolytes.

KEYWORDS
contact ion pair, electrolytes, ionic liquid, pump-probe experiments, solvation species

INTRODUCTION

Ionic liquids (IL) are salts; generally composed of organic cation and organic/inorganic anion and are liquid below 100°C, or even at room temperature, called room-temperature ionic liquids (RTIL). Due to their fascinating physicochemical properties such as low volatility, non-flammability, and high electrochemical and thermal stabilities, ILs are investigated as a suitable solvent system for energy storage and conversion applications, such as supercapacitors, solar cells, and batteries.[1–7] Extensive investigations have been carried out on ILs containing nitrogen-based cations.[8–11] Phosphonium ILs have been the subject of interest in this context.[12–14] For example, a prototype lithium-ion pouch cells using bis(fluorosulfonyl) imide (FSI)-based ionic liquids were designed for space applications and were evaluated for radiation and vacuum tolerance.[15] This was the first IL-lithium ion battery (LIB) to be installed in the "Hodoyashi-3" satellite and was the first IL-LIB to be successfully charged and discharged in orbit.[15] The IL-LIB showed remarkable charge–discharge operation, high g-forces, and extreme vibration tolerance during a rocket launch. However, the high viscosity and cost of ILs are the main drawbacks of IL-based electrolytes.[16,17] Mixing ILs with organic solvents is one of the best strategies to not only reduce the high viscosity and cost of ILs but also improve the transport and electrochemical properties of electrolytes.[17–20]

At present, commercial LIB electrolyte solvents are based on cyclic carbonates mixed with one or more linear carbonates. However, the use of organic solvent electrolytes has two major flaws: (i) the inevitable chemical reactions within the electrolyte decrease the battery lifetime, and (ii) the high inflammability of organic substances increases the risk of fire or explosion. Therefore, developing safe and sustainable novel LIB electrolytes is a crucial

challenge for the current energy storage industry. By mixing RTILs with organic solvents, researchers can take advantage of the high thermal and electrochemical stability of RTILs and high conductivity of organic solvents, which allow the realization of high-performance LIBs.[17–20] However, most of the studies on IL-based electrolytes were dedicated to imidazolium, ammonium, or pyrolidiunium ILs. Recent studies have shown that phosphonium bis(fluorosulfonyl)imide (FSI)-based ILs show superior properties compared to their ammonium analogs, including improved transport properties even at subambient temperature.[12,14,21,22] It has also been reported that methoxy substituted phosphonium cation-based IL have very low viscosity compared to the unsubstituted phosphonium IL.[22]

The solvation structure around the lithium cation and its dynamics play a crucial role in the performance of an LIB. Many studies based on IR, Raman, and NMR Spectroscopy were dedicated to investigating the coordination environment around lithium-ion in electrolytes. However, our understanding of the microscopic environment around Li-ion in high Li salt concentrated ILs is still in the early stages, and there are no reports on solvation structure and dynamics surrounding Li-ion in IL-cosolvent-based electrolytes. In this regard, it has been shown that time-resolved infrared (IR) pump-probe and 2D-IR Spectroscopy can be very useful in addressing the questions related to the solvation structure and dynamics in LIB electrolytes.[23–25] Therefore, to get a better understanding of the molecular solvation structure in IL-cosolvent-based electrolyte, we have investigated the ultrafast dynamics of methylthiocyanate (CH_3SCN) in binary mixtures (in various molar ratios) of the phosphonium IL, namely Tributyl(2-methoxyethyl)phosphonium Bis(trifluoromethanesulfonyl)imide ($P_{444[102]}TFSI$) and methylthiocyanate (CH_3SCN) as a lithium-ion battery electrolyte solvent. We have used Lithium Bis(trifluoromethanesulfonyl) imide (LiTFSI) as a salt in this mixture. Scheme 1 depicts the structure of the IL.

EXPERIMENTAL PROCEDURES

Sample preparation

The IL samples of pure binary mixtures IL + CH_3SCN with the volume ratio of 1:1 and 1:7 (mole ratio of 1:6 and 1:44) were prepared inside a glove box, and LiTFSI salt was added to prepare 1 M and 2 M solutions of LiTFSI in each binary mixture. For linear and nonlinear IR studies, samples were placed in an IR cell assembled with two CaF_2 windows. The optical path length was adjusted by inserting the appropriate Teflon spacer between them.

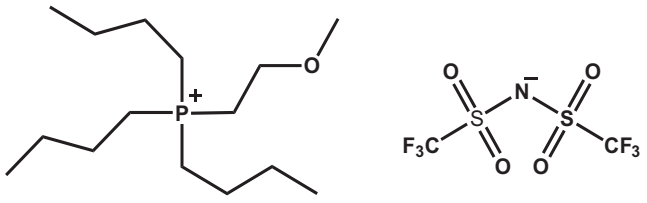

SCHEME 1 Structure of the RTIL Tributyl(2-methoxyethyl) phosphonium Bis(trifluoromethanesulfonyl)imide ([P_{4441O2}] [TFSI])

Steady-state IR absorption

Fourier-transform Infrared (FTIR) spectra were collected with a Perkin–Elmer FTIR spectrometer. FTIR spectra were recorded before and after the IR pump-probe to ensure no degradation of the sample during the experiment.

IR pump-probe spectroscopy

Ti:Sapphire oscillator (Maitai, Spectra Physics) and a regenerative amplifier (Solstice Ace, Spectra Physics) produce 800 nm laser pulses with a repetition frequency of 1 kHz. BBO crystal-based optical parametric amplifier (OPA) system generates two near-IR pulses with wavelengths of approximately 1.3 and 1.9 μm. Mid-IR pulse centered at 2150 cm^{-1} is obtained by the DFG phenomenon by passing near IR pulses through the $AgGaS_2$ crystal. The generated MIR pulse has an approximately 35-fs pulse duration time and about 29 μJ energy. In the polarization selective experiment, the MIR pulse was divided into a probe pulse and a pump pulse using a ZnSe beam splitter (9:1), and the repetition rate of the pump pulse was adjusted to 500 Hz using an electronically synchronized optical chopper. Two-wire grid polarizers were placed before and after the sample in the probe beam. After the interactions of pump and probe pulses with the sample, the probe pulse was divided into parallel and perpendicular polarization components with respect to the pump polarization using ZnSe beam splitter (5:5) and wire grid polarizer. The pump-induced changes in vibrational states in sample molecules can be monitored by the probe pulse, which is measured by monochromator (Horiba, iHR320) and 128(64*2)-element array MCT detector. The parallel polarization component of the probe beam ($S_{\|}$) was detected by the bottom array of the dual array MCT detector. In contrast, the perpendicular polarization component of the probe beam ($S_{\perp}$) was detected by the upper array. The isotropic and anisotropic IR-PP signals are defined as follows in Equations (1) and (2):

$$P(t) = \frac{S_{\|} + 2S_{\perp}}{3}, \quad (1)$$

$$r(t) = \frac{S_{\|} - S_{\perp}}{S_{\|} + 2S_{\perp}} = 0.4C_2(t). \quad (2)$$

Vibrational lifetime and orientational relaxation dynamics are obtained from the $P(t)$ and $r(t)$ decay profiles.

RESULTS AND DISCUSSION

FT-IR Spectroscopy

The IL-CH_3SCN samples were prepared in two different volume ratios of 1:1 and 1:7 (mole ratios of 1:6 and 1:44) named as Samples A and B, respectively. Steady-state FT-IR absorption spectra of A and B, as well as their LiTFSI solutions, are presented in Figure 1. The CN stretching mode of CH_3SCN is observed at 2157 cm^{-1} in pure mixtures (Figure 1a). An increase in absorption of CN stretching mode is observed from A to B as there is an increase in the concentration of CH_3SCN from Samples A to B. With the addition of Li salt, an additional peak at ~2183 cm^{-1} is observed (Figure 1b,c). This peak corresponds to the CN stretching mode of CH_3SCN, which exists as $CH_3SCN\cdots Li^+$ complex form. With the increase of Li concentration, the absorption of the $CH_3SCN\cdots Li^+$ complex peak increases as more Li-ion is available to form a complex with CH_3SCN.

Time-resolved mid-IR pump-probe spectroscopy

Vibrational lifetime analysis

Polarization-selective IR pump-probe experiments have been carried out to selectively determine the vibrational lifetimes and rotational relaxation times of the free and complex form of CH_3SCN. For all LiTFSI sample solutions, the $\upsilon = 0$–1 transition (2157 cm^{-1}) of the nitrile stretching vibration of free CH_3SCN was significantly overlapped with the $\upsilon = 1$–2 transition (2158 cm^{-1}) of the C ≡ N stretching vibration of $CH_3SCN\cdots Li^+$. To avoid such interference, we used the IR PP signals measured at $\omega_t = 2187\ cm^{-1}$ ($\upsilon = 0$–1 transition) for $CH_3SCN\cdots Li^+$ and at $\omega_t = 2137\ cm^{-1}$ ($\upsilon = 1$–2 transition) for free CH_3SCN to obtain the vibrational population relaxation $P(t)$ and orientational relaxation $r(t)$ dynamics. Frequency- and time-resolved IR-PP spectra of the free and complex form of CH_3SCN with the addition of LiTFSI in different binary mixtures of IL-CH_3SCN is shown in Figure S1. It is clear from Figure S1 that the pump-probe signal of the 0–1 vibrational transition of the $CH_3SCN\cdots Li^+$ complex ($\omega_t = 2187\ cm^{-1}$) is contaminated by the pump-induced heating contribution, whereas the 1–2 transition spectra of the free form of CH_3SCN remain almost unaffected. To get the vibrational lifetime of the $CH_3SCN\cdots Li^+$, proper numerical methods were employed to subtract the heating contribution from the measured pump-probe signal.[26] Vibrational population decay patterns of the free (2137 cm^{-1}) and complex form (2187 cm^{-1}) of CH_3SCN for 1 M and 2 M solutions of LiTFSI have been shown in Figure 2. $P(t)$ for the free (2137 cm^{-1}) and complex form of CH_3SCN (2187 cm^{-1}) were fitted with bi-exponential and single exponential decay functions, respectively. The obtained decay times are tabulated in Table 1.

Table 1 shows quite different vibrational lifetimes of free and complex CH_3SCN. Considering the complex composition, including alkyl phosphonium cation, $TFSI^-$, Li^+, and CH_3SCN, it is not surprising that the vibrational dynamics has such complex behavior. The interaction between the CN group and Li-ion is strong enough to produce a large shift in the C ≡ N stretching frequency, as shown in Figure 1. However, due to the alkyl groups around phosphonium cation, FT-IR does not provide clear evidence about the interaction between CH_3SCN and alkyl phosphonium cation. The strong interaction between the CN group and Li-ion also governs the observed vibrational dynamics. Unlike the free CH_3SCN, which shows distinguished T1 and T2 values in binary mixture solutions, the $P(t)$ of $CH_3SCN\cdots Li^+$ can be well fitted with a single exponential function, as shown in Table 1. However, the vibrational lifetime (T1) is sensitive to the relative ratio between IL and CH_3SCN and the concentration of LiTFSI. As stated above, the vibrational dynamics of the CN band in $CH_3SCN\cdots Li^+$ complex form is mainly determined by the interaction between the CN group and Li-ion. Thus, the change in the observed vibrational lifetime can be assigned to the change in Li-ion species rather than the change in the composition around

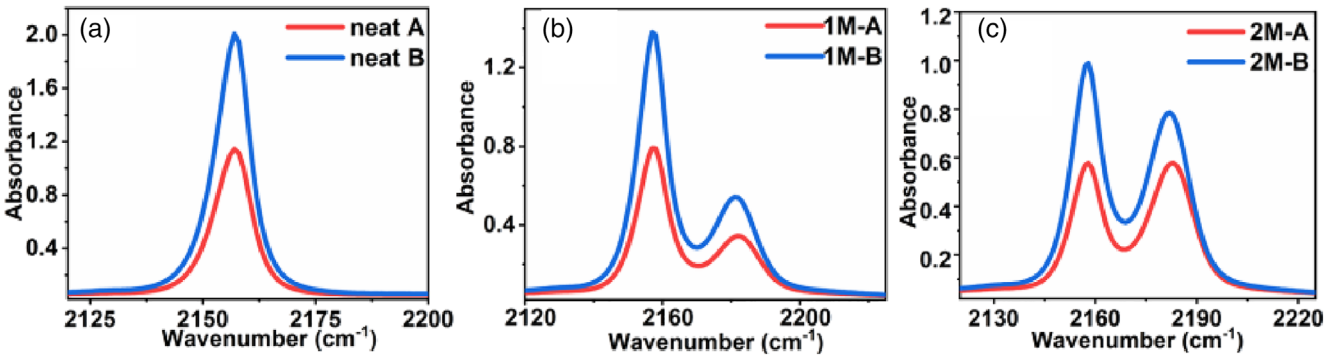

FIGURE 1 CN stretching vibrational peaks of free CH_3SCN in pure binary mixtures (a) and free and complex form of CH_3SCN in solutions of LiTFSI in binary mixtures of IL-CH_3SCN (b and c) with different volume ratios

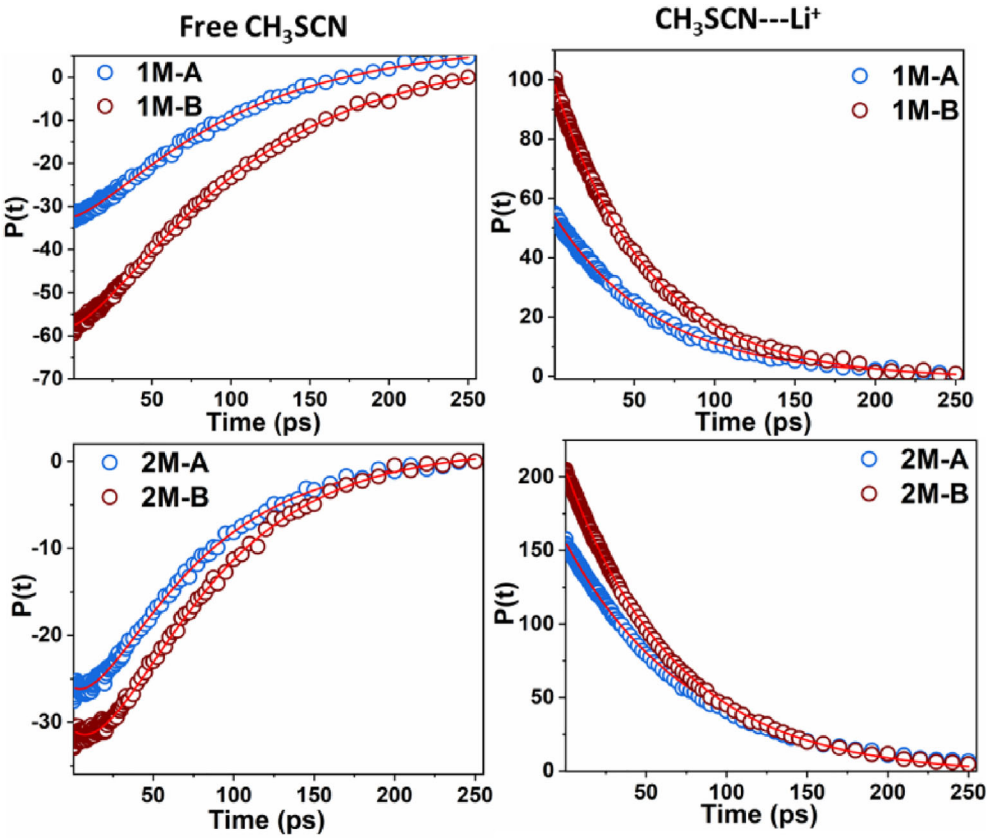

FIGURE 2 Vibrational population decay patterns $P(t)$ of the C ≡ N stretching vibration of free (left panel) and complex (right panel) form of CH_3SCN in solutions of LiTFSI in binary mixtures of IL-CH_3SCN with different volume ratios

TABLE 1 Vibrational lifetimes of the free and complex form of the C ≡ N stretching band of free and complex CH_3SCN

		T1 (ps)	T2 (ps)
Free CH_3SCN	1 M-A	21.7 ± 3.6	95.7 ± 6.2
	1 M-B	27.5 ± 3.5	99.5 ± 5.0
$CH_3SCN\cdots Li^+$	1 M-A	63.7 ± 0.7	
	1 M-B	58.3 ± 0.3	
Free CH_3SCN	2 M-A	19.9 ± 1.9	66.6 ± 3.3
	2 M-B	30.5 ± 3.8	60.7 ± 5.5
$CH_3SCN\cdots Li^+$	2 M-A	77.2 ± 0.7	
	2 M-B	68.6 ± 0.5	

$CH_3SCN\cdots Li^+$. As well known, Li-ion can exist as free Li-ion or contact ion pair Li^+TFSI^-. The increase in salt concentration will make more contact ion pairs. Furthermore, the increase in ionic liquid, [P_{4441O2}] [TFSI], produces more $TFSI^-$ anion in solution, which will decrease the population of free Li-ion due to the common ion effect. In other words, the change in concentration of LiTFSI or relative mixing ratio of IL will cause the change in the amount of contact ion pair. Thus, the complex form can be divided into $CH_3SCN\cdots Li^+$ and $CH_3SCN\cdots Li^+TFSI^-$. With the increase of salt concentration and IL, more $CH_3SCN\cdots Li^+TFSI^-$ species will increase. The measured vibrational lifetime is increased with the increase of LiTFSI contact ion pairs. The neighboring $TFSI^-$ ion will diminish the charge density of Li-ion, which will reduce the interaction strength between CH_3SCN and Li^+ and increase the lifetime. Thus, the vibrational lifetime can resolve the Li^+ solvated only by CH_3SCN and Li^+ in contact ion pair, which is impossible with FT-IR analysis, as shown in Figure 1. However, vibrational dynamics of the CH3SCN-Li^+ complex shows a single exponential decay. Here it should be mentioned that in order to completely resolve the vibrational dynamics of complex form of CH_3SCN, it is important to know the rates of Li^+–CH_3SCN association and dissociation dynamics (chemical exchange dynamics if present), which would also impact the vibrational dynamics of CH3SCN-Li^+TFSI^-. In such a scenario, two-dimensional (2D) IR spectroscopic studies have been shown to be very helpful in calculating the chemical exchange dynamics.[27] Analogous to this study, 2D IR results in present investigation are currently under analysis. At this stage, we are unable to resolve the single exponential vibrational dynamics of $CH_3SCN\cdots Li^+$ complex form.

Unlike $CH_3SCN\cdots Li^+$ species, free CH_3SCN shows distinguished T1 and T2 values in binary mixture solutions with 1 M and 2 M LiTFSI. Two decay times indicate that there are at least two different solvation structures around CH_3SCN. Within the experimental error limits, T1 values are increased from ∼21 ps to ∼29 ps with the

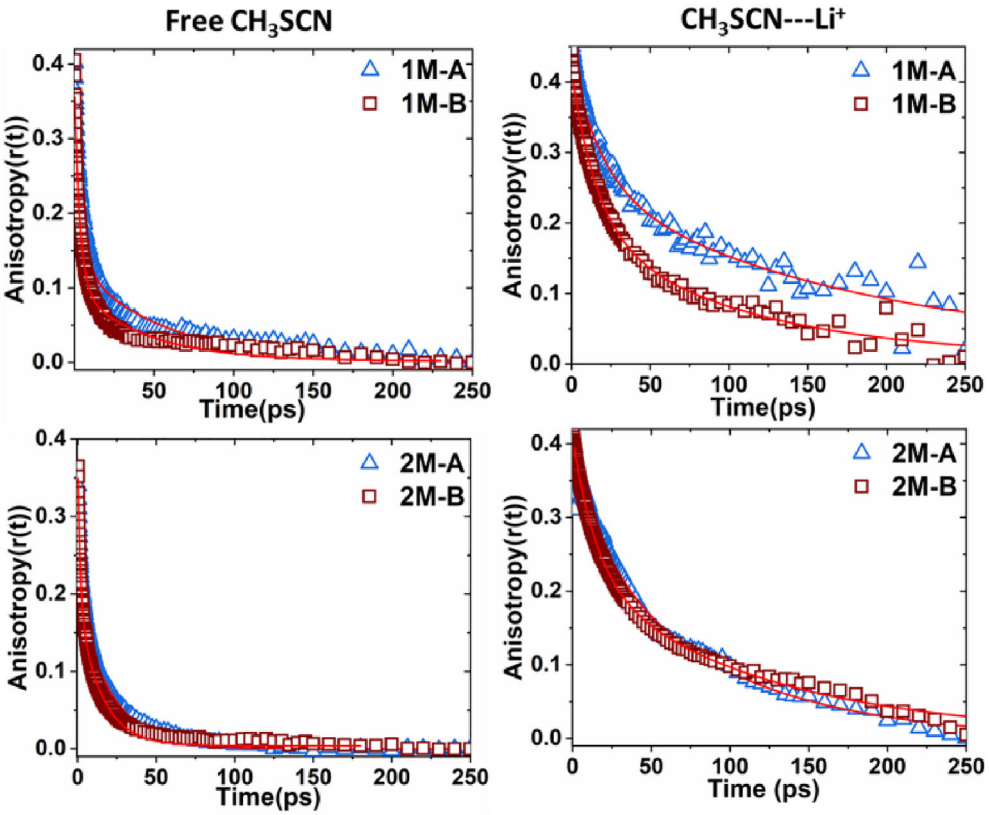

FIGURE 3 IR-PP anisotropic decay pattern of the free and complex form of CH_3SCN in solutions of LiTFSI in binary mixtures of IL-CH_3SCN with different volume ratios. The red lines are a bi-exponential fit

TABLE 2 Rotational relaxation time constant of the free and complex form of CH_3SCN in solutions of LiTFSI in binary mixtures of IL-CH_3SCN with different volume ratios

		τ_1 (ps)	τ_2 (ps)
Free CH_3SCN	1 M-A	4.36 ± 0.14	55.3 ± 2.0
	1 M-B	3.75 ± 0.10	43.7 ± 3.1
$CH_3SCN\cdots Li^+$	1 M-A	19.42 ± 1.50	170 ± 11.0
	1 M-B	15.94 ± 0.69	102 ± 5
Free CH_3SCN	2 M-A	1.85 ± 0.01	21.70 ± 0.30
	2 M-B	1.61 ± 0.02	14.80 ± 0.30
$CH_3SCN\cdots Li^+$	2 M-A	20.85 ± 1.60	86.95 ± 2.90
	2 M-B	15.13 ± 0.40	116.20 ± 2.50

increase of CH_3SCN from A to B irrespective of salt concentrations. However, T2 values show totally different trends of change with the increase of Li salt concentrations and CH_3SCN in solution. T2 values do not show a clear dependence on the increase of CH_3SCN but decrease significantly with the increase of salt concentration. Due to the weak interaction strength, CH_3SCN surrounding with other CH_3SCN cannot be distinguished from CH_3SCN interacting with alkyl phosphonium cation ($[P_{4441O2}]$) with FT-IR analysis, as shown in Figure 1. Previously the vibrational lifetime of CH_3SCN in acetonitrile was measured as ~92 ps,[27] which is close to our measurement (~97.5 ps) in 1 M solution. Based on this, we could assign T2 coming from CH_3SCN surrounding with other CH_3SCN and T1 from CH_3SCN interacting with $[P_{4441O2}]$. Vibrational lifetime with corresponding weighting factor has been provided in Table S1. It can be seen from Table S1 that the weighting factors A1 and A2 do not change significantly with increase in the either CH_3SCN or LiTFSI salt concentration. It can also be concluded from A2 values in Table S1 that the vibrational lifetime component of CH_3SCN surrounded by other CH_3SCN molecules (T2) is the major contributor (80%–90%) towards the overall vibrational lifetime of free CH_3SCN. The observed increase of T1 from A to B is correlated with the decrease in relative population of alkyl phosphonium cation ($[P_{4441O2}]$). Also, the significant decrease of T2 is related to the increase in salt concentration. The further study combined with MD simulation will reveal the molecular origin of this correlation. Such an observation demonstrates that infrared pump-probe experiments become an essential tool to investigate the molecular species that exist in complex IL-based LIB electrolytes.

Rotational dynamics analysis

We have also analyzed the anisotropic decay patterns, $r(t)$, of the free and complex form of CH_3SCN at the same

wavelength used for vibrational lifetime analysis. As shown in Figure 3, all measured anisotropic decay patterns were fit well with a bi-exponential function. The obtained two decay times are presented in Table 2.

As shown in Table 2, both free and complex from of CH_3SCN show bi-exponential decay behavior, which indicates that the microenvironment of both free and complex from of CH_3SCN is heterogeneous in nature. Parts of the observed change in rotational relaxation time constants can be explained based on Stokes–Einstein–Debye equations.[28] First, rotational dynamics of the $CH_3SCN\cdots Li^+$ is slower than the free CH_3SCN in all the samples, which indicated that the rotation of $CH_3SCN\cdots Li^+$ is more hindered due to the increase of the effective hydrodynamic volume of the rotator. Second, with the increase of CH_3SCN (from A to B), rotational dynamics of free CH_3SCN has been observed to be faster due to a decrease in the viscosity of the medium. The detailed explanation about the assignment of each rotational relaxation time to molecular behavior requires MD simulations. Instead, we will show that the rotational dynamics has the potential to reveal various solvation species, which cannot be resolved with linear FT-IR Spectroscopy. As shown in Section 3.2.1, the vibrational lifetime analysis suggests the presence of at least four different solvation species. Free CH_3SCN showing a single peak in FT-IR analysis consists of CH_3SCN surrounding with other CH_3SCN and interacting with alkyl phosphonium cation ($[P_{4441O2}]$). Complex $CH_3SCN\cdots Li^+$ is a mixture of CH_3SCN interacting with free Li-ion and CH_3SCN interacting with Li^+ in contact ion pair, Li^+TFSI^- which cannot be distinguished with FT-IR analysis.

Considering the volume of the rotator, the faster τ_1 observed in free CH_3SCN could be assigned as CH_3SCN surrounding with other CH_3SCN and the slower one τ_2 as CH_3SCN interacting with $[P_{4441O2}]$. Corresponding weighing factors for rotational relaxation time constants for the free and complex form of CH_3SCN have been provided in Table S2. It can be observed from Table S2 that with increase in CH_3SCN (from A to B), for free CH_3SCN, relative contribution from τ_1 (A1) increases and τ_2 (A2) decreases which is understandable as with increasing CH3SCN concentration, relative population of the alkyl phosphonium cation ($[P_{4441O2}]$) decreases. Such a clear trend was not observed in comparing the vibrational lifetime components of free CH_3SCN (Section 3.2.1). Furthermore, the observed rotational relaxation time in complex $CH_3SCN\cdots Li^+$ also can also be divided into two classes, $CH_3SCN\cdots Li^+$ and $CH_3SCN\cdots Li^+TFSI^-$. Compared to the vibrational lifetime analysis, which showed only single time component for complex $CH_3SCN\cdots Li^+$, rotational relaxation studies for the same shows two distinct time component with significant contribution from both classes, $CH_3SCN\cdots Li^+$ and $CH_3SCN\cdots Li^+TFSI^-$ (Table S2). Considering the bulky size of $TFSI^-$ as shown in Scheme 1, two distinguished decay times are understood based on Stokes–Einstein–Debye equations. This is fascinating because rotational dynamics could provide more detailed information about the solvation structure, which cannot be resolved in FT-IR analysis. Furthermore, the distinction between $CH_3SCN\cdots Li^+$ and $CH_3SCN\cdots Li^+TFSI^-$ becomes clear compared to the analysis with the vibrational lifetime, which requires the comparison through the increase or decrease of LiTFSI contact ion pairs.

CONCLUSION

This study has provided interesting observations about structure and dynamics in a phosphonium IL-CH_3SCN-based electrolyte system. A significant difference in vibrational dynamics of the free CH_3SCN and $CH_3SCN\cdots Li^+$ complex and their corresponding rotational dynamics have been observed in different IL-CH_3SCN mixtures. The vibrational lifetime analysis indicates an increase in the population of Li^+TFSI^- contact ion-pair with the increase of salt concentration and IL. Hence, more $CH_3SCN\cdots Li^+TFSI^-$ species will increase, which in turn leads to an increase in the vibrational lifetime of $CH_3SCN\cdots Li^+$. The observed increase of T1 with the increase in the concentration of CH_3SCN can be correlated with the decrease of alkyl phosphonium cation ($[P_{4441O2}]$). The bi-exponential nature of the vibrational population relaxation indicates that CH_3SCN is distributed in a heterogeneous environment. With the increase in Li concentration, the T2 values for free CH_3SCN decreases for a particular composition of IL and CH_3SCN. This also indicates that the microenvironment of the two solutions is heterogeneous in nature. However, the further study combined with MD simulation may provide a detailed picture of the molecular origin of this correlation. Rotational dynamics of free CH_3SCN becomes faster with the increase in the concentration of CH_3SCN. Interestingly rotational dynamics of the free, as well as the complex form of CH_3SCN, becomes faster with the increase in Li concentration in a particular solvent mixture. This indicates a deviation from the linear viscosity dependence of the rotational dynamics. Rotational relaxation studies clearly point out toward the presence of two distinct complex forms of CH_3SCN, that is, $CH_3SCN\cdots Li^+$ and $CH_3SCN\cdots Li^+TFSI^-$ with comparable contribution toward overall rotational relaxation time of the $CH_3SCN\cdots Li^+$ complex. Analysis of the rotational dynamics in the light of the Stokes–Einstein–Debye hydrodynamic model further clarifies the presence of at least four different solvation species; CH_3SCN surrounding with other CH_3SCN, CH_3SCN interacting with alkyl phosphonium cation $([P_{4441O2}]^+$, CH_3SCN interacting with Li-ion and $CH_3SCN\cdots Li^+TFSI^-$. The study reveals that the environment of free CH_3SCN and $CH_3SCN\cdots Li^+$ complex changes drastically with the change in CH_3SCN mole fraction and Li salt concentration in the mixture. This, in turn, can impact the Li-ion transport property significantly in the IL-based electrolyte.

ACKNOWLEDGMENTS

This research was supported by a grant from the Institute for Basic Science (IBS-R023-D1) and by the National

Research Foundation of Korea (NRF) grant funded by the Korea government (MSIT) (NRF-2020R1A5A1019141).

CONFLICT OF INTERESTS

The authors declare that there are no conflict of interests.

REFERENCES

[1] M. Armand, F. Endres, D. R. MacFarlane, H. Ohno, B. Scrosati, *Nat. Mater.* **2009**, *8*, 621.
[2] D. R. MacFarlane, N. Tachikawa, M. Forsyth, J. M. Pringle, P. C. Howlett, G. D. Elliott, J. H. Davis, M. Watanabe, P. Simon, C. A. Angell, *Energy Environ. Sci.* **2014**, *7*, 232.
[3] H. Sakaebe, H. Matsumoto, K. Tatsumi, *Electrochim. Acta* **2007**, *53*, 1048.
[4] H. Nakagawa, Y. Fujino, S. Kozono, Y. Katayama, T. Nukuda, H. Sakaebe, H. Matsumoto, K. Tatsumi, *J. Power Sources* **2007**, *174*, 1021.
[5] A. Guerfi, M. Dontigny, P. Charest, M. Petitclerc, M. Lagacé, A. Vijh, K. Zaghib, *J. Power Sources* **2010**, *195*, 845.
[6] L. Lombardo, S. Brutti, M. A. Navarra, S. Panero, P. Reale, *J. Power Sources* **2013**, *227*, 8.
[7] M. Watanabe, M. L. Thomas, S. Zhang, K. Ueno, T. Yasuda, K. Dokko, *Chem. Rev.* **2017**, *117*, 7190.
[8] P. C. Howlett, D. R. MacFarlane, A. F. Hollenkamp, *Electrochem. Solid-State Lett.* **2004**, *7*, A97.
[9] H. Matsumoto, H. Sakaebe, K. Tatsumi, M. Kikuta, E. Ishiko, M. Kono, *J. Power Sources* **2006**, *160*, 1308.
[10] G. B. Appetecchi, M. Montanino, S. Passerini, *ACS Symp. Ser.* **2012**, *1117*, 67.
[11] S. A. Mohd Noor, P. C. Howlett, D. R. Macfarlane, M. Forsyth, *Electrochim. Acta* **2013**, *114*, 766.
[12] K. Tsunashima, Y. Sakai, M. Matsumiya, *Electrochem. Commun.* **2014**, *39*, 30.
[13] K. J. Fraser, D. R. MacFarlane, *Aust. J. Chem.* **2009**, *62*, 309.
[14] G. M. A. Girard, M. Hilder, H. Zhu, D. Nucciarone, K. Whitbread, S. Zavorine, M. Moser, M. Forsyth, D. R. MacFarlane, P. C. Howlett, *Phys. Chem. Chem. Phys.* **2015**, *17*, 8706.
[15] M. Yamagata, K. Tanaka, Y. Tsuruda, Y. Sone, S. Fukuda, S. Nakasuka, M. Kono, M. Ishikawa, *Electrochemistry* **2015**, *83*, 918.
[16] G. A. J. Giffin, *Mater. Chem. A* **2016**, *4*, 13378.
[17] F. U. Shah, O. I. Gnezdilov, R. Gusain, A. Filippov, *Sci. Rep.* **2017**, *7*, 16340.
[18] P. M. Bayley, G. H. Lane, N. M. Rocher, B. R. Clare, A. S. Best, D. R. MacFarlane, M. Forsyt, *Phys. Chem. Chem. Phys.* **2009**, *11*, 7202.
[19] T. Vogl, S. Menne, A. Balducci, *Phys. Chem. Chem. Phys.* **2014**, *16*, 25014.
[20] L. Aguilera, J. Scheers, A. Matic, *Phys. Chem. Chem. Phys.* **2016**, *18*, 25458.
[21] K. Tsunashima, A. Kawabata, M. Matsumiya, S. Kodama, R. Enomoto, M. Sugiya, Y. Kunugi, *Electrochem. Commun.* **2011**, *13*, 178.
[22] K. Tsunashima, M. Sugiya, *Electrochem. Commun.* **2007**, *9*, 2353.
[23] J. Lim, K.-K. Lee, C. Liang, K.-H. Park, M. Kim, K. Kwak, M. Cho, *J. Phys. Chem. B* **2019**, *123*, 6651.
[24] K.-K. Lee, K. Park, H. Lee, Y. Noh, D. Kossowska, K. Kwak, M. Cho, *Nat. Commun.* **2017**, *8*, 14658.
[25] X. Chen, K. D. Fulfer, K. T. Woodard, D. G. Kuroda, *J. Phys. Chem. B* **2019**, *123*, 9889.
[26] Y. L. Rezus, H. J. Bakker, *J. Chem. Phys.* **2006**, *125*, 144512.
[27] Y. Kwon, S. Park, *Phys. Chem. Phys.* **2015**, *17*, 24193.
[28] C. Hu, R. Zwanzig, *J. Chem. Phys.* **1974**, *60*, 4354.

SUPPORTING INFORMATION

Additional supporting information may be found in the online version of the article at the publisher's website.

How to cite this article: P. K. Sahu, J. Kim, K. Park, E. Kim, S. Mondal, K. Kwak, M. Cho, *Bull. Korean Chem. Soc* **2022**, *43*(2), 215. https://doi.org/10.1002/bkcs.12463